A Monte Carlo Study of Titrating Polyelectrolytes in the Presence of Salt

Magnus Ullner* and Bo Jönsson†

Physical Chemistry 2, Chemical Center, University of Lund, P.O. Box 124, S-221 00 Lund, Sweden

Received February 26, 1996; Revised Manuscript Received July 1, 1996[⊗]

ABSTRACT: Monte Carlo simulations have been performed for two simple models of a titrating polyelectrolyte: (i) a rigid rod and (ii) a freely jointed chain. Both models have fixed bond lengths, and the polyelectrolyte charges interact through a screened Coulomb potential. Chains consisting of 80−1000 monomeric units have been studied at three salt concentrations: 0.001, 0.01, and 0.1 M. Conformational properties and the apparent dissociation constant are reported as functions of chain length, chain ionization, monomer−monomer bond length, and salt concentration. Mean field expressions are compared to the simulation results and are, in general, found to be excellent approximations for the rigid rod, but they are also able to provide semiquantitative descriptions of the apparent dissociation constant for the freely jointed chain. Comparisons with experimental data show that the conformational properties of the flexible model can reproduce features of the titration curves, although the use of a screened Coulomb potential overestimates the response to changes in salt concentration.

Introduction

Proteins, colloids, membranes, and flexible polymers are all examples of the charged macromolecules and molecular assemblies covered by the term polyelectrolyte. Here we will concentrate on so-called weak polyelectrolytes, polymers with titrating groups whose charge varies with the pH of the solution. We use a simple model, containing only the basic features of a linear chain of titrating sites that interact only through a fixed bond length and a screened Coulomb potential. Only occasionally is there an additional constraint on the monomers, in the form of hard spheres. Though admittedly simplified, this model allows us to study fairly long polymers and, in particular, the electrostatic effects.

To simulate the titrating behavior, we use a grand canonical ensemble with a fixed bulk chemical potential for the protons, which lets the ionization of the chain vary and respond to the Coulomb interactions as the conformations change as well as establishing correlations between different sites. This technique has also been used for linear polyelectrolytes by Reed and Reed[1] for a three-state rotational isomeric model and by Sassi *et al.*[2] for a cubic-lattice model, which also included short-range attractive interactions. Another method that has been used by others is to perform the simulations in the canonical ensemble with a partial but fixed degree of ionization.[3−7]

Simulation algorithms performing global moves markedly improve convergence characteristics for global properties like the average end-to-end separation compared to conventional methods using only single-monomer moves. The pivot algorithm[8,9] has allowed us to simulate chains with several thousand monomers, and we have previously reported the results for the salt-free case.[10,11] This study is a continuation of that work, incorporating salt as a screening of the Coulomb potential. The models and simulation technique are the same and are described only briefly here.

Over the years, various rigid models have been employed in the discussion of simulated or experimental titrations. In the salt-free case, we used a mean field approximation of the rigid rod with discrete charges. Here, we have derived its screened Coulomb counterpart explicitly, to show how the number of monomers enters into the expression. The size-independent form has been used previously by Manning[12] and Cleland *et al.*[13] More well-known, perhaps, is the cylinder with a uniform surface charge immersed in an electrolyte described by the Debye−Hückel approximation.[14−16] Manning has used an expression that is the low salt limit of both the infinite rigid rod and a particular infinite line model with a uniform charge.[17−19] We have compared these analytical expressions, which differ in mathematical complexity but very little in the numerical results over their range of validity.

We have also searched the literature for experimental results that correspond to our simulations. Since the simulations do not contain any attractive interactions, there are no sharp conformational transitions. We therefore want systems that are "coil-like" in the whole range of ionization. Unfortunately, experimental data are not abundant. Usually, only one group has studied a particular system and reports only one set of results per case. An exception is polyacrylic acid, which has been thoroughly studied by Kawaguchi and Nagasawa[20] and Mandel.[21] Comparisons are also made with poly-DL-glutamic acid,[22] carboxymethyl cellulose,[23] and hyaluronic acid.[16] The simulations give a salt dependence that is too strong. We have therefore solved the nonlinearized Poisson−Boltzmann equation for the charged cylinder, which is the preferred approach according to Nagasawa and co-workers.[15,24] We also consider excluded volume effects.

All of the above models treat the salt ions in a mean field way, and neither Debye−Hückel nor Poisson−Boltzmann theory is expected to give reliable results in the presence of multivalent counterions. There are indications, however, that Debye−Hückel theory is a valid approximation in the case of a 1:−1 salt and a not too highly charged polyelectrolyte,[4,25] and the use of the Poisson−Boltzmann equation would extend the validity to higher charge densities.

* Author to whom correspondence should be addressed. E-mail: fk2mul@dix.fkem2.lth.se.
† E-mail: fk2boj@grosz.fkem2.lth.se.
⊗ Abstract published in *Advance ACS Abstracts,* August 15, 1996.

S0024-9297(96)00309-9 CCC: $12.00

Simulation Models

Titrating sites are joined by rigid bonds to form a linear polyelectrolyte. Model 1 is a rigid rod, while model 2 still has rigid bonds but the chain is flexible, i.e., it is allowed to bend. The sites will be considered to be acidic, implying zero charge in the protonated state and one negative unit of charge in the deprotonated state. Furthermore, the polyelectrolyte is infinitely diluted, and thus only intramolecular interactions are considered. The solvent water is treated as a continuum which screens the Coulomb potential with a dielectric constant $\epsilon_r = 78.3$. Salt ions are implicitly represented via the Debye screening parameter κ. In the case of a 1:−1 salt, κ is given by $\kappa = (2e^2 N_A C_s/\epsilon_r \epsilon_0 k_B T)^{1/2}$, where e is the elementary charge, C_s the salt concentration, ϵ_0 the permittivity of vacuum, N_A Avogadro's number, k_B Boltzmann's constant, and T the temperature.

Except for an extension of model 2, where all monomers have been given a hard-sphere diameter (distance of closest approach) of 3 Å, nonbonded monomers interact only through the screened Coulomb potential. Two uncharged sites may therefore occupy the same position in model 2, and the total energy is given by

$$E_C = \frac{e^2}{4\pi\epsilon_r\epsilon_0}\sum_{i}^{N}\sum_{j>i}^{N}\frac{z_i z_j \exp(-\kappa r_{ij})}{r_{ij}} \tag{1}$$

where N is the number of monomers, r_{ij} is the distance between monomers i and j, and z_i is the amount of charge on monomer i (either 0 or −1).

Monte Carlo Simulations

The Monte Carlo (MC) simulations are performed as described previously[10,11] using the Metropolis algorithm.[26] Chain conformations are sampled with a pivot algorithm.[8,9] A monomer i is chosen, and the rest of the chain, monomers $i+1$ to N, is then rotated as a rigid body around one of the coordinate axes with monomer i as origin. This greatly improves the sampling efficiency compared to just moving one monomer at a time and allows simulations of very long chains with several thousand monomers.

The acidic behavior is investigated in a grand canonical ensemble. A monomer is picked at random, and an attempt is made to switch its charge state. The change in (free) energy, ΔE, governing the success of the attempt, is composed of the change in the screened Coulomb interactions between monomers, ΔE_C, and the free energy change corresponding to the acid−base reaction of an isolated monomer,

$$\Delta E = \Delta E_C \pm k_B T \ln 10(\mathrm{pH} - \mathrm{p}K_0) \tag{2}$$

where pH is the pH of the bulk, and pK_0 is the intrinsic pK_a of a monomer. The difference $\mathrm{pH} - \mathrm{p}K_0$ is an input parameter of the program. The plus sign is used when the monomer is to be protonated, and the minus sign is used when it is to be deprotonated. Protons are exchanged only with the bulk, as intramolecular moves are more time consuming and do not affect the averages.

A conformational change is attempted once in every 20 steps (model 2). In all other steps, a change in the charge state is tried. The total number of steps is around 10^8. Every run is preceded by an equilibration of 10^5−10^6 steps, where a change in conformation is attempted every other step, starting from a straight line with a charge on every other monomer.

Results and Discussion

The electrostatic interactions between charged monomers oppose the dissociation of the protons, shifting the equilibrium toward the acidic (uncharged) form of the monomers. Expressed in another way, the effective pK_a of a monomer will be higher than the intrinsic dissociation constant pK_0, the dissociation constant of an isolated monomer. The average effect over the whole molecule can be measured, e.g., by potentiometric titration as an elevated apparent dissociation constant,

$$\mathrm{p}K = \mathrm{pH} - \log\frac{\alpha}{1-\alpha} \tag{3}$$

where $\alpha = \langle(1/N)\sum_{i=1}^{N}\alpha_i\rangle$ is the overall degree of dissociation. The apparent dissociation constant, which corresponds to treating the polyacid as an effective monoacid, is not a constant but increases with α due to increasing electrostatic repulsion. The repulsion will be strengthened by shorter bond lengths, more compact conformations, and lower salt concentrations (a lower degree of screening).

The excess free energy, F, due to the interactions between the monomers is directly related to the difference between the apparent and intrinsic dissociation constants,

$$\Delta\mathrm{p}K = \mathrm{p}K - \mathrm{p}K_0 = \frac{1}{Nk_BT\ln 10}\frac{\partial F}{\partial\alpha} = \frac{1}{\ln 10}\frac{\partial\tilde{F}}{\partial\alpha} \tag{4}$$

where the tilde indicates a division by Nk_BT.

The major effect of the salt is a screening of electrostatic interactions, making the Coulomb energy per monomer and ΔpK independent of N for large enough concentrations. Longer bonds lower the required salt concentration. An increasing degree of ionization will also affect the chain conformations. This is demonstrated, for example, by an expansion of the radius of gyration or the end-to-end separation, R_{ee}. The latter is defined as

$$R_{ee}{}^2 = \langle r_{1N}{}^2\rangle \tag{5}$$

The Rigid Rod. As in the salt-free case, the rigid rod may be described using a mean field approximation where the charge is distributed evenly along the rod. With a (fractional) charge on each monomer equal to the overall degree of dissociation, α, the electrostatic energy per monomer is approximated by

$$\tilde{E} = \frac{\langle E_C\rangle}{Nk_BT} = \frac{l_B\alpha^2}{N}\sum_{k=1}^{N-1}(N-k)\frac{e^{-\kappa ka}}{ka}$$
$$= \frac{l_B}{a}\frac{\alpha^2}{N}\sum_{k=1}^{N-1}\left(\frac{N}{k}-1\right)(e^{-\kappa a})^k \tag{6}$$

where $l_B = e^2/4\pi\epsilon_r\epsilon_0 k_B T$ is the Bjerrum length (in the simulations, which were performed at 298 K, $l_B \approx 7.16$ Å). The second part of the sum is a geometric series. Taking the limit of infinite chain length gives

$$\sum_{k=1}^{N-1}(e^{-\kappa a})^k = \sum_{k=0}^{N-1}(e^{-\kappa a})^k - 1 \rightarrow$$
$$\frac{1}{1-e^{-\kappa a}} - 1 = \frac{1}{e^{\kappa a}-1}, \quad N\rightarrow\infty \tag{7}$$

The first part of the sum can be identified as an integral over a geometric series:

$$\sum_{k=1}^{N-1}\frac{(e^{-\kappa a})^k}{k} = \sum_{k=1}^{N-1}\int_0^{e^{-\kappa a}} t^{k-1}\,dt$$

$$= \int_0^{e^{-\kappa a}}\sum_{l=0}^{N-2} t^l\,dt \rightarrow$$

$$\int_0^{e^{-\kappa a}}\frac{1}{1-t}\,dt = -\ln(1-e^{-\kappa a}), \quad N\rightarrow\infty \quad (8)$$

The resulting expression for the Coulomb energy is

$$\tilde{E}_{MF} = -\frac{l_B}{a}\frac{\alpha^2}{N}\left[N\ln(1-e^{-\kappa a}) + \frac{1}{e^{\kappa a}-1}\right] \quad (9)$$

Figure 1 contains a comparison between the exact electrostatic energy and the mean field value, eq 9, for a rigid rod. The chain has no conformational freedom, and the whole difference is due to charge−charge correlations along the rod. The correlation contribution is comparatively small, and the largest discrepancy, seen for $\alpha = 0.5$, is only a few tenths of a k_BT.

The Coulomb energy is also the excess free energy since there is no entropy, because in the mean field treatment of the rigid rod, both the charge distribution and the chain conformation are fixed. Combining eqs 4 and 9 gives

$$\Delta pK_{MF} = -\frac{2}{\ln 10}\frac{l_B}{a}\frac{\alpha}{N}\left[N\ln(1-e^{-\kappa a}) + \frac{1}{e^{\kappa a}-1}\right] \quad (10)$$

Note that an infinite number of monomers is only used to obtain the limiting values of convergent sums, and the second term in the parentheses reflects the fact that the chains are finite. This term is needed to give the proper N dependence for short chains at low salt concentrations. In the least-screened case presented here, $a = 3$ Å and $C_s = 1$ mM, only about 100 monomers are needed to make the second term one-tenth of the first one. If it is very long chains that are of primary interest, it is reasonable to drop the second term, which simplifies the expression to

$$\Delta pK_{MF} = -\frac{2}{\ln 10}\frac{l_B}{a}\alpha\ln(1-e^{-\kappa a}) \quad (11)$$

The mean field approximation is similar to that of Reed and Reed for *all-trans* conformations of models with fixed bond angles,[1] where the rigid rod can be considered as a special case ($\theta = 0°$ in their notation), which allows an analytical expression. This size-independent form has also been used by Manning[12] and Cleland *et al.*[13]

Figure 2 shows a comparison of ΔpK for a rigid rod obtained from simulations and the mean field theory, where we have used the full expression for ΔpK_{MF}, eq 10. The agreement is quite good and shows that the correlation term is of minor importance; for a chain with $a > 6$ Å, it is almost zero. Note that the difference in ΔpK tends to zero as α tends to 1, at least for the longer chains. This is in contrast to the salt-free case, where a positive difference remains at $\alpha = 1$.[11] In both cases, the mean field approximation gives the correct energy in this limit (cf. Figure 1), but here the assumption that the sites are equivalent is valid since the screening removes the end effects. When the chain is fully charged, there is not much room for any other type of correlation, and the entropic contribution vanishes.

The nearest-neighbor correlation can be taken into account using an Ising model.[27] If the nearest-neighbor

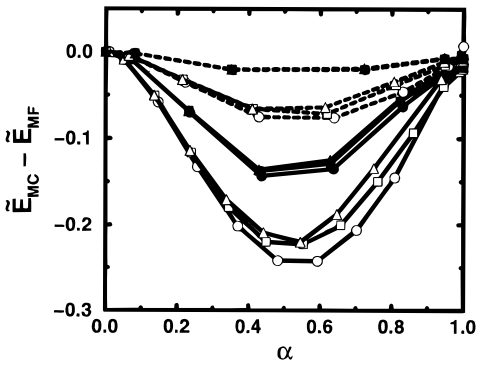

Figure 1. Plot of the difference in Coulomb energy between MC simulation and the mean field theory (eq 9) as a function of α for rigid rods (model 1) with bond lengths, a, of 3 (solid lines) and 6 Å (dashed lines) and numbers of monomers N = 80 (circles), 320 (squares), and 1000 (triangles). Open and filled symbols represent salt concentrations of 0.001 and 0.1 M, respectively. $\tilde{E}_{MC}$ values for the fully charged rod at these salt concentrations are 8 and 3.1, respectively, when $a = 3$ Å and 3.3 and 0.9 when $a = 6$ Å.

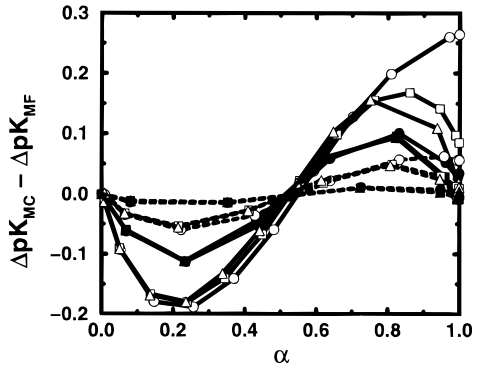

Figure 2. Plot of the difference in ΔpK between MC simulation and the mean field theory (eq 10) as a function of α for rigid rods (model 1). Line types and symbols are the same as in Figure 1. ΔpK_{MC} values when $\alpha \approx 1$ and $a = 3$ Å are 7 and 2.7 at salt concentrations of 0.001 and 0.1 M, respectively. For $a = 6$ Å, the corresponding values are 2.9 and 0.8.

interactions are treated explicitly and all other interactions are treated as above, we get a correction to the mean field result:

$$\Delta pK_{MFI} = \Delta pK_{MF} + \frac{(2\alpha-1)w}{\ln 10} + \log\frac{[\sqrt{4\alpha(1-\alpha)(e^{-w}-1)+1}+2\alpha-1](1-\alpha)}{[\sqrt{4\alpha(1-\alpha)(e^{-w}-1)+1}-2\alpha+1]\alpha} \quad (12)$$

where

$$w \equiv \frac{l_B}{a}e^{-\kappa a}$$

The correction term is zero for $\alpha = 0$, 0.5, and 1.0. This means, in particular, that it does not affect any correlation error at $\alpha = 1$, but it reduces the error elsewhere by approximately halving the period of the oscillations in the difference between simulation and theory. To be more specific, the difference between simulation and eq 12 vanishes and changes sign approximately where the difference for the bare mean field approximation has two extrema. This results in a (shifted) maximum difference that is about half that of the bare mean field when $a = 3$ Å, and for $a = 6$ Å the reduction factor is 5. In absolute terms, the gain is less impressive: a

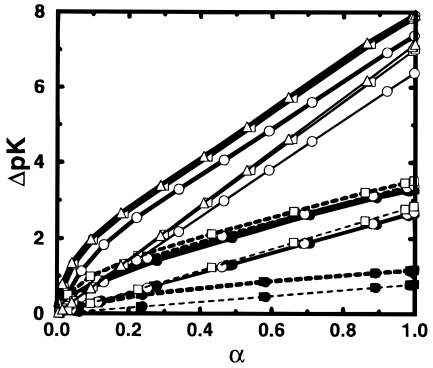

Figure 3. Plot of the shift in the dissociation constant as a function of α for flexible chains (model 2). Line types and symbols are the same as in Figure 1, using lines of normal thickness for Monte Carlo data and thin lines for the mean field rigid rod approximation, eq 10. Note that the curves for $a = 3$ Å, $C_s = 0.1$ M and $a = 6$ Å, $C_s = 0.001$ M coincide.

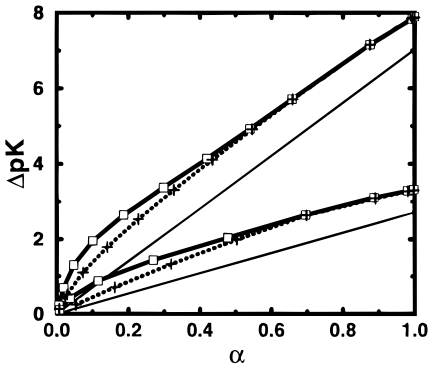

Figure 4. Plot of the shift in the dissociation constant as a function of α for flexible chains (model 2) with pointlike monomers (solid lines, □) and hard-sphere monomers (dotted lines, +). The bond length a and the hard-sphere diameter are both 3 Å, and the number of monomers is 320. Salt concentrations are 0.001 (top) and 0.1 M (bottom). Thin lines without symbols represent the rigid rod approximation, eq 10.

reduction from 0.05 to 0.01 pK units in the latter case when the salt concentration is 0.001 M, for instance. It is questionable if it is worth the increased mathematical complexity.

Manning has suggested that the rigid rod should be treated as a linear lattice with an effective lattice spacing;[12] i.e., rather than give each site the effective charge α, $N\alpha$ unit charges should be equally spaced along the rod, with a neighbor separation of a/α. This approximation is inferior to the one we have used, giving about a 5-fold increase in the maximum error.

The Flexible Chain as an Effective Rigid Object. Encouraged by the good behavior of the mean field theory, we will now go one step further and compare the mean field rigid rod results with the simulated ΔpK for a flexible chain (model 2). In doing so, we should, of course, not expect a quantitative agreement, since the rigid rod represents the limiting case of a fully stretched chain, and in Figure 3 it is clear that the approximate expression always underestimates the shift in the dissociation constant for the flexible chains. The absolute difference will decrease with increasing salt concentration, but the relative difference will increase because the chain will be less expanded and therefore less rodlike. What we hope to find is that the general behavior is well described by the mean field approximation. In this respect, Figure 3 is a comforting sight. We have already commented that the N dependence is weak, but when the bond length is as short as 3 Å and the salt concentration is as low as 0.001 M, the 80-mer stands out from the 320-mer and 1000-mer, which, on the other hand are rather close. This is mirrored in the plot of eq 10. The simulations show that chains with $a = 3$ Å at $C_s = 0.1$ M behave almost like chains with $a = 6$ Å at $C_s = 0.001$ M. This is also reflected in the approximate curves. For now, we may say that the rigid rod approximation describes the dependence on N, a, and C_s rather well. We will make this more quantitative below.

When it comes to the α dependence, our theory predicts a linear dependence for ΔpK, but the simulations have a more complex behavior. In the beginning of the charging process, the chain is Gaussian; a newly arrived charge runs a considerable risk of finding itself in the proximity of other charges, and there is a steep increase in ΔpK. As more charges are accumulating, the chain responds by adopting more extended conformations, which counteracts the rise in ΔpK; the slope decreases and almost levels off. Though the curves are never really linear, it is a reasonable approximation to regard them as straight lines above some value of α. Judging by Figure 3, a rough estimate would be $\alpha > 0.2$. If the polyelectrolyte had been pre-exanded, e.g., by excluded volume interactions or as a result of a good solvent, the initial rise would be less pronounced, and the chain behavior would be more rodlike. This is displayed in Figure 4, where model 2, which has pointlike monomers, is compared to a hard-core cousin, where each monomer is a hard sphere with a 3 Å diameter. The two models differ only at low values of α. When the amount of charge is large, the electrostatic interactions dominate and the curves coincide. If, on the other hand, there had been an effective attraction, e.g., due to a poor solvent, the deviations from rigid rod behavior would have been even greater. There could even be a conformational transition like the helix−coil transition of poly-L-glutamic acid.[22] It is interesting to note that the nonlinearity of a titration curve is not necessarily due to a break-down of the Debye−Hückel approximation, which would make the screened Coulomb potential invalid and call for some other theory, like the solution of the nonlinearized Poisson−Boltzmann equation (see below). Conformational behavior and interactions besides the electrostatic one can play an important role, even though the major effect may be electrostatic in origin. Charge correlations within the polyelectrolyte also give rise to deviations from a linear dependence on α, as we saw in the rigid rod case, but these effects are comparatively minor.

Other elongated rigid objects, besides the rigid rod with discrete charges, have also been proposed as models for polyelectrolytes. Hill calculated the electrostatic free energy for both spherical and cylindrical models using the Debye−Hückel approximation.[14] One of these is an infinite cylinder with the charge uniformly smeared over the surface, which leads to

$$\Delta pK_{CS} = \frac{2 l_B Z_l}{\ln 10}\left[\frac{K_0(\kappa a)}{\kappa a K_1(\kappa a)} + \ln\frac{a}{b}\right] \qquad (13)$$

where $K_n(x)$ is a modified Bessel function of the second kind, b is the radius of the cylinder, a is the radius of closet approach of the mobile ions to the cylinder, and Z_l is the number of unit charges per unit length. To compare this expression to the simulations and the rigid rod, we only use one length, a, to describe the polyelectrolyte model. First, we set $a = b$ since there are no

explicit ions in the simulations. Second, we take the charge density Z_l to be α/a, which is the same as the total charge divided by a contour length Na. This parameter reduction seems like a reasonable first guess, even in an experimental situation.

Manning and Holtzer[17,18] have advocated a model that can be interpreted as a low salt approximation to a uniformly charged, infinite line where the titrating charge is put in the solution at a radial distance a from the line, though this is not the way it is presented. The starting point is the electrostatic potential at the distance a, given the seemingly ubiquitous Debye–Hückel approximation. Using this directly would give

$$\Delta pK_{CL} = \frac{2l_B Z_l}{\ln 10} K_0(\kappa a) \tag{14}$$

For $\kappa a \ll 1$, $K_0(\kappa a) \approx -\ln \kappa a$, and

$$\Delta pK_{LL} = -\frac{2l_B Z_l}{\ln 10} \ln \kappa a \tag{15}$$

The authors arrive at this expression after a small detour, where they let $a \to 0$ in order to make the above approximation, remove the (singular) ln a term, and then put it back again as a self-energy term with a finite radius a. This allows them to discuss alternative self-energy terms, but the expression used in the end is the one corresponding to eq 15. The prescription for Z_l given by the authors is the same as the one we used above, i.e., total number of unit charges divided by the maximum length of the polyion. Here, we will again use length a for the radius as well as the distance between the charges. Equation 15 is also the limiting expression of the (infinite) rigid rod, eq 11, when $\kappa a \ll 1$. This fact was used by Manning at a later date to justify the logarithmic line expression.[19] This limit is not very restrictive when a is small. With intercharge distances of 3 and 6 Å, it corresponds to $C_s \ll 1$ M and $C_s \ll 0.26$ M, respectively.

The rigid rod is, of course, best described by the rigid rod approximation, but what about a flexible chain? If we want to approximate it as a rigid object, should we use the rigid rod, the cylindrical surface, or the "cylindrical line"? The answer is that it does not really matter. With the same linear charge density and the same value of the length parameter a, there is not much of a numerical difference, as can be seen in Figures 5 and 6. The only exception is the logarithmic version of the cylindrical line, eq 15, which gives negative values of ΔpK when $\kappa a > 1$, i.e., for large a and high salt concentrations. This "breakdown" should not come as a surprise since the equation is based on the assumption that $\kappa a < 1$. If this approximation is not made and the Bessel function is kept as in eq 14, the behavior is very close to that of the rigid rod.

The consensus of the models is perhaps not so surprising, either. After all, the three models are very closely related. They are all elongated, rigid objects immersed in a dielectric continuum described by Debye–Hückel theory. As long as the linear charge density is based on the contour length, they all predict that ΔpK is linear in α. In the comparisons with simulation, we have used Z_l of the rigid rod, i.e., α/a, and the bond length as the length parameter a. As we discussed in the context of the rigid rod, this leads to an underestimation of ΔpK. In Figures 5 and 6, this is indicated by the filled symbols, which represent ΔpK at $\alpha \approx 1$. We also suggested that the simulated ΔpK

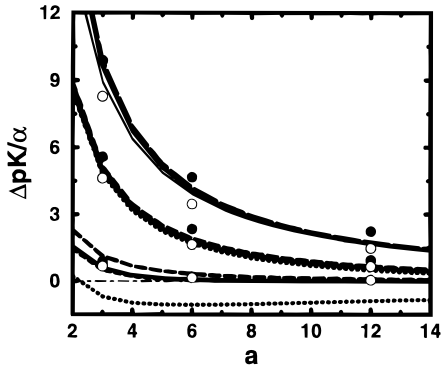

Figure 5. Length parameter dependence of ΔpK for simulations and theoretical models. Symbols represent Monte Carlo results: ●, ΔpK at $\alpha \approx 1$; ○, the slope of ΔpK *vs* α obtained by linear regression using the data at $\alpha > 0.2$. Solid lines show the predictions of the rigid rod model with the size-dependent version, eq 10, as a thin line and the infinite N approximation, eq 11, which is more comparable to the other models, having normal thickness. The logarithmic line (eq 15), the cylindrical line (eq 14), and the cylindrical surface (eq 13) are drawn with dotted lines, dashed lines, and long-dashed lines, respectively. The dot-dashed line marks $y = 0$. The salt concentrations are, from top to bottom, 0.0001, 0.01, and 2 M.

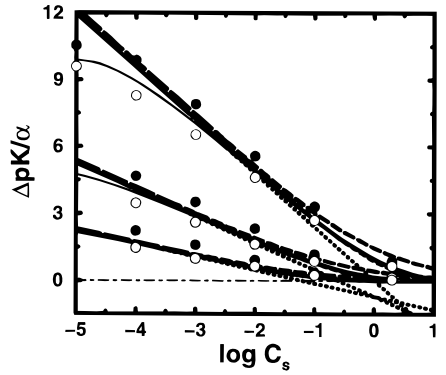

Figure 6. Salt concentration dependence of ΔpK for simulations and theoretical models. Line types and symbols are the same as in Figure 5. The bond length parameters a are, from top to bottom, 3, 6, and 12 Å.

dependence on α could be approximated as linear for $\alpha > 0.2$, and in Figures 5 and 6, this slope, obtained by linear regression, is plotted using open symbols. Now the models overestimate the simulation data. Though the agreement is not quantitative, it is not far wrong in either case, which is quite good considering the crudeness of the models. The agreement can, of course, be improved by treating a as a fitting parameter, which is often done in comparisons with experiment. More interesting is, perhaps, that the models describe the dependence on a and C_s quite well, the exception still being the logarithmic version of the cylindrical line.

In principle, it is possible to partly account for the flexibility (and nonlinearity) by using an effective charge density like the total charge divided by the end-to-end distance. The Monte Carlo results easily lend themselves to such a test. The verdict is that the new approximation overestimates ΔpK and underestimates its slope, the opposite of the original situation. Thus, the added complexity does not seem to be warranted. A probable reason is that the length scales in the theories do not have any exact counterparts in the real systems; they are effective values. We have already seen that it makes little difference if we think of a as a charge–charge distance or as a cylinder radius. Experimenters have to decide which starting point gives the best

agreement in most cases. Actually, as can be seen below, experimental results leave this question unanswered. One reason is that there is some flexibility in assigning values for the parameters, and another is that there are deviations from the behavior predicted by the models using the Debye−Hückel approximation and a single length parameter.

Leaving the question about the underlying descriptions and approximations for the moment, the biggest difference between the models is the mathematical complexity or, rather, the complexity of numerical calculation. It may not be of great importance in this day and age, when there is a computer on almost every desktop, but there is still a sense of convenience in the ability to reach for the personal pocket calculator. The modified Bessel functions of eqs 13 and 14 can, therefore, be a deterrent, while the logarithms and exponentials of the rigid rod and the logarithmic line do not pose any problems in this respect. The latter is simpler than the former but has a limited range of validity. For very low values of κa, where $e^{-\kappa a} \approx 1 - \kappa a$, the logarithmic line, eq 15, can, of course, be used instead of eq 11, but in this limit the N dependence will start to show if the chain is not very long, and the size-corrected eq 10 may be a better approximation. On the other hand, the interaction between different chains may also become significant and make the use of any of the above expressions questionable. This is also the case if the polyelectrolyte concentration is too high.

Simulations vs Experiments. We have now made a thorough investigation of different rigid models in the light of our flexible simulated model. The question is, of course, how well the latter describes reality. Does it reproduce experimental results? A direct comparison with experiment is difficult for several reasons. Real systems are usually polydisperse, although this should not be a major problem. The degree of polymerization for a typical polyelectrolyte, like polyacrylic acid, is normally larger than the few hundred monomers needed to remove any significant size effects (cf. the discussion after eq 10). Experimental measurements are always performed at finite polymer concentrations, where both the polyelectrolyte and its counterions contribute to the screening. This needs to be taken into consideration, but when titration curves are published, it has usually been confirmed that dilution does not affect their features or relative behavior.

It is also difficult to translate the separation between charged groups in a partly branched chain into our single size parameter a. In our model, it should be the distance between neighboring charges. The correspondence in the results between the flexible chain and the rigid rod indicates that it is the maximum local separation, i.e., the local most extended conformation, that is the key. We have made a very crude analysis with the help of a plastic model building kit to find reasonable values for a. We have, of course, displayed the simulations that give the best agreement with experiment, but a is not optimized more than to within 1 Å.

Another immediate concern is the choice of pK_0. Experimentally, it can be obtained by extrapolating the titration data to $\alpha = 0$, but without data close to this point it usually not clear what the curve should look like in this region. An alternative is to use the pK of the monomers or a similar compound, e.g., an oligomer, and correct for the salt concentration. This is shown to be "extremely hazardous" by Mandel.[21] Whichever method is used, there may be scatter among the experimental results, themselves, making it hard to say anything conclusive (cf. Figure 7). For no other reason than to be consistent, we have used our own extrapolations of the experimental curves, except for Mandel's data, where we had to rely on his polynomial fit. Looking at his examples of titration curves, the fits seem reasonable also for pK_0.

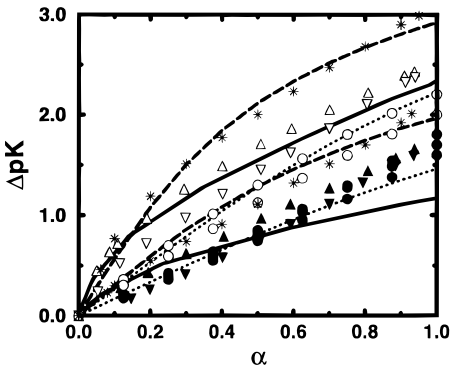

Figure 7. ΔpK as a function of α for experiments, theory, and simulations. Symbols represent experimental data for polyacrylic acid, with open symbols used for 0.01 M salt and filled symbols for 0.1 M. Triangles are points measured from Figure 1 of Kawaguchi and Nagasawa.[20] Triangles pointing up represent the isotactic form, and those pointing down are for the syndiotactic one. The circles are plotted directly using the parameters for a fitted second-order polynomial tabulated by Mandel.[21] Solid lines are simulations of flexible chains with 320 monomers and a bond length of 6 Å, with the low-salt case on top. The dotted lines are solutions to the full Poisson−Boltzmann equation for a cylinder with a 2 Å radius and a linear charge separation (inverse linear charge density) of 6.6 Å. These parameters were obtained by a crude fitting of the experimental points lowest in α to eq 13, the solution to the linearized equation. Solutions to the full equation with the parameters used by Kawaguchi and Nagasawa, 5.5 and 2.06 Å, respectively, are drawn with dashed lines. The stars are data for atactic PAA from Figure 4 of Nagasawa *et al.*[29] pK_0 was obtained by extrapolation to $\alpha = 0$, except in the case of Mandel's data, which were taken as they are in Table 2 of his article.

Next comes the quest for experimental data. Unfortunately, extensive studies of suitable systems seem to be very scarce in the literature. A suitable system is one in which there is a monotonic variation of pK with α, unlike the helix-to-random coil transition displayed by poly-L-glutamic acid.[22] We have found one system in which there is more than one independent study and more than one curve per salt concentration, polyacrylic acid (PAA). Figure 7 shows the results for 0.01 and 0.1 M salt from Kawaguchi and Nagasawa[20] and Mandel[21]. At high salt concentration, there is excellent agreement between the two experimental groups, while at low salt concentrations there is some difference. This may be explained partly by the choice of pK_0, as already discussed. Also shown are the results for simulations of the flexible model with $a = 6$ Å. The agreement with experiments seems to be quite good, especially for Kawaguchi and Nagasawa's measurements with 0.01 M added salt. There is one observation that seems to be a general conclusion from these comparisons with experiment. The models discussed so far give too strong a salt dependence with the present treatment. They are all based on the Debye−Hückel approximation, and an immediate explanation is that the assumption of a linear response implied by the use of a screened Coulomb potential is not valid when the polyelectrolyte is highly charged.

Kotin and Nagasawa[24] and Nagasawa and Holtzer,[15] for example, have advocated solving the full Poisson−

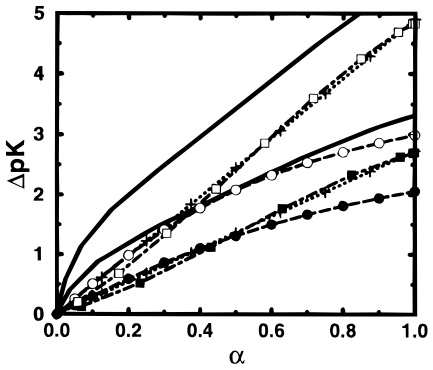

Figure 8. ΔpK as a function of α when $a = 3$ Å for theories and simulations. Solid lines represent simulations of the flexible model, and the dot-dashed curves with squares are simulations of the rigid rod. The mean field rod (eq 11) is displayed as dotted lines with plus signs. The results are for 320 monomers and a bond length of 3 Å. Dashed curves with circles are solutions to the Poisson−Boltzmann equation for a cylinder in which both the radius and the linear charge separation (inverse linear charge density) are 3 Å. The salt concentration for the upper curves is 0.01 M (open symbols), and that for the lower one is 0.1 M (filled symbols).

Boltzmann equation, which takes care of some of the nonlinear effects:

$$\nabla^2\psi = -\frac{eN_A}{\epsilon_r\epsilon_0}\sum_i z_i C_i \exp\left(\frac{-z_i e\psi}{k_B T}\right) \qquad (16)$$

where $\psi = \psi(\mathbf{r})$ is the electrostatic potential at the point $\mathbf{r}$, z_i the valency of salt species i, and C_i its bulk concentration. Since a rigid rod or a charged cylinder is able to describe the high α behavior of a flexible chain in the Debye−Hückel picture, it seems reasonable to also use a cylinder in solving the Poisson−Boltzmann equation. With only a 1:−1 salt and cylindrical symmetry, the equation "simplifies" to

$$\frac{1}{r}\frac{d}{dr}\left(r\frac{d\psi}{dr}\right) = -\frac{eN_A C_s}{\epsilon_r\epsilon_0}\left[\exp\left(\frac{-e\psi}{k_B T}\right) - \exp\left(\frac{e\psi}{k_B T}\right)\right] \qquad (17)$$

where r is the distance from the center of the cylinder. In the mean field picture, ΔpK is the interaction between the proton and the potential at the titrating site. If b is the radius of the cylinder and the position of a new proton charge, we get

$$\Delta pK = -\frac{1}{\ln 10}\frac{e\psi(b)}{k_B T} \qquad (18)$$

To get a picture of the differences between the Poisson−Boltzmann solution, the mean field rigid rod, the simulated rigid rod, and the flexible model, we have plotted their results for two single length parameters, 3 and 6 Å, in Figures 8 and 9, respectively, for the salt concentrations in question. At low charge densities (low potential), the Poisson−Boltzmann equation can be linearized, and the cylindrical surface (eq 13 with eq 18) is a solution. At low α, the solutions give the same result as the rigid rod, and when $a = 6$ Å, the difference is small everywhere. In fact, the disagreement seen in Figure 9 at $C_s = 0.1$ M is really the difference between the cylindrical surface and the rigid rod. At high charge densities, the situation is more dramatic: the Poisson−Boltzmann equation gives a screening that is much larger than the Debye−Hückel approximation, especially at low salt concentrations. When $a = 3$ Å and α

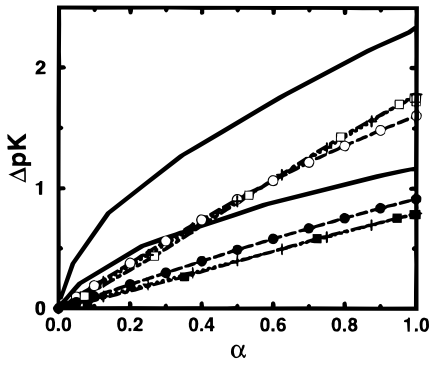

Figure 9. ΔpK as a function of α when $a = 6$ Å for theories and simulations. This figure is the same as Figure 8, except that the length parameters of the models are 6 Å. Note that the y-axis scale is also twice that of Figure 8.

$= 1$ at $C_s = 0.01$ M, the former gives a ΔpK about 2 pK units lower than the rigid rod. As we noted earlier, the effect of flexibility is to give an initial rise in ΔpK, but otherwise the behavior is closely related to that of the rigid models.

Returning to PAA, we have just seen that the solutions to the full Poisson−Boltzmann equation with both the radius and the linear charge separation set to 6 Å give results very similar to those for the rigid rod over the whole range of α. This charge density is thus not big enough to give any larger deviations from a linear response. A length parameter of 6 Å implies that neighboring charges are as far apart as possible, and the value is close to the upper limit even in that respect. The model-building kit gives an estimate for the upper distance between 5 and 6 Å, where the lower value is more appropriate for the isotactic form. In the literature, 2.5 Å is sometimes quoted as a normal charge separation.[18,28] This corresponds to the distance between two monomers along the backbone. Kawaguchi and Nagasawa used 2.06 Å and a cylinder radius of 5.5 Å when solving the Poisson−Boltzmann equation.[20] These parameters give a high enough charge density to invoke a nonlinear response and a reduced salt dependence at large α. However, a substantial curvature not seen in the experimental curves is also introduced. In fact, at high salt concentrations, the experimental curves tend to become concave up (positive curvature) rather than concave down. Figure 7 also shows the ΔpK values obtained with the Poisson−Boltzmann equation and the parameters of Kawaguchi and Nagasawa. Viewed like this, there does not seem to be much agreement. One explanation is the problem in determining pK_0. To show that the parameters are not unreasonable, we have also added data for atactic PAA obtained by Nagasawa and co-workers at an earlier date.[29] Now there is very good agreement. The salt dependence, measured as the shift in pK due to salt at $\alpha \approx 1$, is of the same order as that of the other rigid models, i.e., around 1 pK unit. Their experimental value is 0.8, while Mandel gets values between 0.2 and 0.6.

Noting that Debye−Hückel is the low charge limit of Poisson−Boltzmann, we may use the first experimental points at low α to estimate the cylinder parameters with the help of the cylindrical surface. In an effort to negotiate all the curves, we get a charge separation of 6.6 Å, which is too big, and a cylinder radius of 2 Å, which is close to the distance between the charge centers of the carboxyl groups and the backbone of PAA in an extended (model kit) conformation. When we use these parameters in the Poisson−Boltzmann equation, the

agreement becomes quite good, especially when compared to Mandel's data (Figure 7). Fitting can sometimes be a questionable procedure, and these results may say more about the flexibility of the Poisson−Boltzmann equation than about physical reality. If the separation is large and the radius small, the curves become less curved, which may be the mathematical reason for the increased agreement. Still, the parameters obtained are not unreasonable, and we fitted only one end of the curves with a limiting expression and were nevertheless able to get good results for the entire range using the full equation.

So far, we have neglected the excluded volume with respect to salt. This will also effect the salt dependence. At low salt concentrations the effect is minor, but at higher salt concentrations a more substantial amount of salt is excluded and unable to screen. The result is an increased apparent dissociation constant. This would help the flexible model ($a = 6$ Å) by keeping the low-salt curve (which is in good agreement with experiment) relatively fixed, while lifting the high-salt curve. This model does not contain any distance of closest approach for salt ions, nor does the rigid rod, but the cylindrical surface does. Until now, we have set the parameter equal to the radius of the cylinder, but by relaxing this constraint, we can calculate the size of the effect within the Debye−Hückel approximation. Let us start from a cylinder with all length parameters set to 6 Å, since it should have roughly the same relative behavior as the flexible chain with $a = 6$ Å. In the nonexcluded case, the ΔpK values at $\alpha = 1$ are 1.91 and 1.00 at 0.01 and 0.1 M salt concentration, respectively. The radius of an ion is 2−3 Å, and we could also expect some contribution from the polyelectrolyte itself (the charge is "below the surface"). With radii of exclusion of 8 and 10 Å (the charge is still at $b = 6$ Å), we get 1.96/1.12 and 2.01/1.23, respectively. Thus, we see that the correction is of the order of tenths of a k_BT and that the correction grows more than twice as fast with the distance of closest approach at the higher salt concentration. This is enough to at least improve the agreement in Figure 7.

We have already noted the change in appearance of the experimental curves when the salt concentration is increasing, going from concave down to concave up. The results actually tend to look more like those of the rigid rod at high salt concentrations. This is perhaps not all that surprising, considering that PAA is very soluble in water. Water thus acts as a good solvent, and the chain should be rather extended, even at low degrees of dissociation. This is in contrast to the simulations, where the starting point for the titration is a more compact conformation. As a comparison, polymethacrylate, which is less soluble, displays a larger negative curvature and even a conformational transition.[29] Based on this, we can propose a third explanation, which at the same time takes care of the strong salt dependence and the changing features of the PAA curves. If the chain is "pre-expanded" the electrostatic interactions at high salt concentrations may not be enough to expand it any further, and it acts like an effective rigid rod. The 0.1 M data are in perfect agreement with a rigid rod that has a bond length of 4 Å. When there is less screening, the electrostatic interactions may take effect and expand the chain. This would give curves that are concave down according to the simulations. Furthermore, the effective, maximum charge separation would increase, and so would the bond length of the flexible

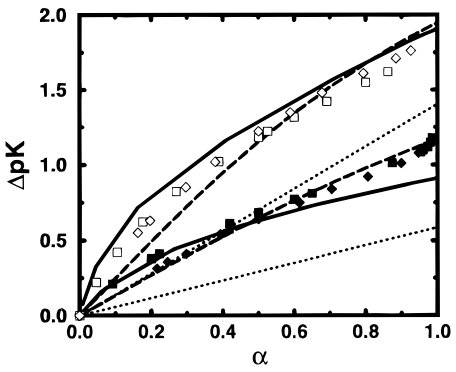

Figure 10. ΔpK as a function of α for experiments, theory, and simulations. Symbols represent experimental data, with open symbols used for 0.01 M salt and filled symbols for 0.1 M. Squares represent data for poly-DL-glutamic acid, and the points were obtained from Figure 1 of Olander and Holtzer.[22] Diamonds are carboxymethyl cellulose points measured by Muroga *et al.* and subsequently measured by us from their Figure 1.[23] Solid lines are simulations of flexible chains with 320 monomers and a bond length of 7 Å. The dotted lines are the mean field rigid rod equivalents (eq 11) of the simulations, and the dashed lines denote solutions to the Poisson−Boltzmann equation for a cylinder with a 5 Å radius and a linear density of one charge per 5 Å. pK_0 was obtained by extrapolation to $\alpha = 0$.

model that best fits the data. This supports the fact that the flexible chain with $a = 6$ Å agrees very well with experiments in Figure 7 for $C_s = 0.01$ M, but less so for $C_s = 0.1$ M. We are now allowing our model parameters to change as well, which may be a bit dubious. Keeping the length parameter fixed, a chain that is expanded with the help of interactions in addition to the electrostatic ones, e.g., covalent interactions, excluded volumes, or a good solvent, is expected to have a titration behavior intermediate between those of the freely jointed chain and the rigid rod. It is possible to sandwich the experimental data with the results of the flexible chain and the rigid rod at these two salt concentrations, but the strong salt dependence, which we have alluded to before, would most probably let the experimental data escape even such a crude prediction at concentrations outside this range.

None of the mechanisms proposed to improve the agreement, nonlinear salt correlation, excluded volume, and changing conformational behavior, exclude any of the others. We should, perhaps, look at a case in which some of these effects are expected to have less influence. If we choose a system with a lower charge density, the deviations from a linear response in the ion atmosphere should be smaller. If the polyelectrolyte is less soluble, but unable to perform a sharp conformational transition, the range of flexibility should be more like our simulated model. Such a case is that of poly-DL-glutamic acid. We know that the stereoregular poly-L-glutamic acid contracts and forms a helix when the charge density is low. Although poly−DL−glutamic acid is not able to form a regular α-helix in the same way, it does have the same tendency to contract,[22] thus leaving room for the chain to expand when the electrostatic interactions increase. If we use our plastic model kit once again and try to optimize the charge separation, we get a linear charge density of 1 charge every 4 Å and an intercharge distance of 8−10 Å for nearest and next-neighbors. In Figure 10, we have the flexible chain with $a = 7$ Å, together with experimental data for poly-DL-glutamic acid from Olander and Holtzer.[22] There are also results for carboxymethyl cellulose from Muroga et al.,[23] which happen to be extremely similar to those for poly−DL−

glutamic acid. Now the curves are concave down, with the largest curvature at low α as predicted by the flexible model. With a bond length of 7 Å, we once again get good agreement for 0.01 M salt and less so at 0.1 M, which would be helped by excluded volume effects, both within the chain and with respect to salt. The former would even out the curvature at low α, and the latter would increase ΔpK relatively more at 0.1 M salt.

If we play the game of fitting the Poisson−Boltzmann solutions at low α, we run into trouble. The large curvature makes it hard to tell where to apply the tangents for the Debye−Hückel approximation. In principle, we should calculate the slope at $\alpha = 0$, but we lack points close enough. From the very first points, we are also able to get parameters that are straining the limits of what is physically acceptable. A compromise is a cylinder with a 5 Å radius and an equally large inverse linear charge density. These are reasonable values. The plastic model also gives 5 Å as the distance between the backbone and the side-chain charge. The overall agreement with experiment is slightly better than that for the simulations, but the line shapes are not as good in that they have the largest curvature at high values of α, although carboxymethyl cellulose does behave that way at 0.1 M salt. Remember that the cylinder is a rigid model. We therefore conclude that the high curvature at low α seen in the experiments can, indeed, be attributed to flexibility. Note that the Poisson−Boltzmann solutions, in general, need shorter length parameters than the flexible model to get a correct absolute shift in the apparent dissociation constant. This is also due to the rigidity of the cylinder. The "one-length" Poisson−Boltzmann corresponds to the rigid rod at low charge densities (cf. Figure 9) and is therefore expected to underestimate the shift, if the length parameters were to be set equal to the bond length of the flexible model. The simulated model, of course, gets its stronger interactions from the flexibility, which makes it less extended than the rigid rod, since it has to fight entropy to expand. The corresponding rigid rod is also shown in Figure 10.

In a study of hyaluronic acid, Cleland *et al*. found reasonable agreement between experiments and the cylindrical surface model when 10 Å was used for both the linear charge density and the radius.[16] Later, Cleland also made comparisons with the rigid rod model with $a = 10$ Å and found similar agreement.[13] He then noted that, while 10 Å is larger than the expected radius of 4−7 Å, it is exactly the distance between neighboring charges, the parameter expected on the basis of the rigid rod model. This indicates that the polymer is rather extended, even in its low charge state, and perhaps is better viewed as a rod of discrete charges than as a cylinder with a smeared surface charge. The latter is apparent from an atomic picture but not as clear from a mathematical description, as we have already discussed.

Manning has, for a long time, proposed an alternative way to treat nonlinear effects, through the by-now famous counterion condensation.[17−19,12] In his later work, he describes the counterions as territorially bound. Such an ion atmosphere that can be attributed to the polyelectrolyte also appears in the solutions to the Poisson−Boltzmann equation.[24,30] At high charge densities, the Debye−Hückel approximation underestimates the amount of net counter charge in the vicinity of the polyelectrolyte and overestimates the field at the titrating sites. From the point of view of the better approximation, the Poisson−Boltzmann equation, the deviations increase gradually as the charge density increases. Manning treats this as a partition equilibrium that sets in at a certain critical charge density, $\xi = l_B/b = 1$, where b is the linear charge separation (inverse density) or lattice spacing. The critical behavior introduces discontinuities not observed in experimental titration curves. Manning is, of course, aware of this, and some of his defense can be read in refs 19 and 12.

Structural Properties. As the chain gradually ionizes, it responds by expanding. In the salt-free case, it is possible, at least in principle, to set up a balance between the chain entropy and the electrostatic interactions, since the latter are global. This is the basis of the Flory approach, which we have applied with modest success in the past.[10,11] We have also shown that there, in fact, exist universal scaling laws, at least for our freely jointed chain (model 2), although we were not able to unveil any exact mathematical formulation.[11]

When there is salt present, the situation is more complex. The screening makes the electrostatic interactions local, and there may be a local competition with the chain entropy, while other mechanisms may act on a global scale. At very high salt concentrations, we expect the global behavior to be that of a chain consisting of hard spheres or excluded volume interactions, i.e., the end-to-end distance should grow as $N^{3/5}$.[31]

Such an N dependence also results from a simple Flory approach using the following arguments. For the energetic term we will use a spherical Ansatz with an even monomer distribution. This means that the charge density is $3\alpha Ne/4\pi R^3$, with R being the radius. If $R \gg \kappa^{-1}$, most monomers are unaware of the surface. All they see is a uniform charge density, and we get N identical interaction integrals where we can extend the upper limit to infinity:

$$\tilde{E} = {}^1/_2 \int_0^\infty \frac{3\alpha^2 N}{4\pi R^3} \frac{l_B \exp(-\kappa r)}{r} 4\pi r^2 \, dr = \frac{3 l_B \alpha^2 N}{2 R^3 \kappa^2} \qquad (19)$$

To get the free energy, we add the elastic or entropic term as usual:[11,32]

$$\tilde{F} = \frac{3 l_B \alpha^2 N}{2 R^3 \kappa^2} + {}^3/_2 \left(\frac{R}{Na}\right)^2 \qquad (20)$$

Finally, we get the variational solution by minimizing with respect to R:

$$R = \frac{(3 l_B)^{1/5} \alpha^{2/5} N^{3/5} a^{2/5}}{\kappa^{2/5}} = \text{const} \times \alpha^{2/5} N^{3/5} C_s^{-1/5} a^{2/5} \qquad (21)$$

In Figure 11, the simulated end-to-end separation is compared to the above result. The true functional form is clearly more complex than the simple power law, but still the agreement is surprisingly good. To get a more quantitative assessment of the approximate exponentials, we have calculated the slopes of ln R_{ee} against the logarithms of the different variables. The results, which are not to be taken too literally since most exponents are based on as few as three points, some even just two, are displayed in Tables 1−4. Indeed, the N dependence tends to the expected $N^{3/5}$ behavior for long bonds and high salt concentrations. Also, the other exponents

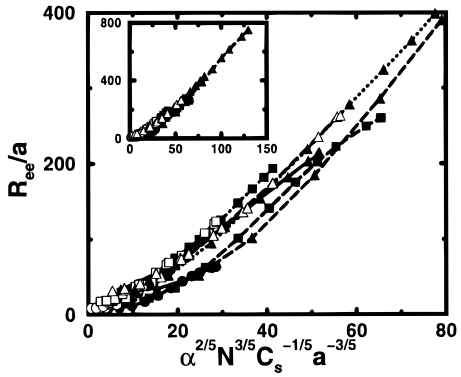

Figure 11. Scaled end-to-end separation as a function of $\alpha^{2/5}N^{3/5}C_s^{-1/5}a^{-3/5}$ for flexible chains (model 2) with 80 (circles), 320 (squares), and 1000 (triangles) monomers at salt concentrations of 0.001 (dashed lines), 0.01 (dotted lines), and 0.1 M (solid lines). Filled symbols are used for bond lengths of 3 Å, and open symbols are used for $a = 6$ Å.

Table 1. R_{ee} Approximated as a Power Law: α-Exponents[a]

		a/Å		
C_s/M	*N*	3	6	12
0.001	80	0.60	0.66	0.65
	320	0.50	0.62	0.58
	1000	0.52		0.53
0.010	80	0.57	0.59	0.52
	320	0.55	0.53	0.49
	1000	0.52		0.46
0.100	80	0.54	0.47	0.39
	320	0.48	0.45	0.40
	1000	0.46		0.38

[a] The value predicted by eq 21 is 0.4. $\alpha \geq 0.2$ was used to avoid the Gaussian chain behavior close to $\alpha = 0$.

Table 2. R_{ee} Approximated as a Power Law: *N*-Exponents[a]

		α			
C_s/M	*a*/Å	0.25	0.50	0.75	1.0
0.001	3	1.01	0.98	0.97	0.98
	6	0.99	0.96	0.95	0.94
	12	0.82	0.79	0.80	0.76
0.010	3	0.83	0.80	0.79	0.80
	6	0.80	0.78	0.76	0.75
	12	0.69	0.68	0.67	0.66
0.100	3	0.70	0.68	0.66	0.66
	6	0.67	0.68	0.66	0.65
	12	0.59	0.62	0.62	0.62

[a] The value predicted by eq 21 is 0.6.

predicted by the Flory approach are remarkably good, considering the crudeness of both the variational approximation and the calculation of the exponents. It is just the *a* dependence that seems to be slightly off, an exponent of 0.3 rather than 0.4 at 0.1 M salt.

It is possible that the agreement will deteriorate outside of the range of values used here. There are some indications that 0.01−0.1 M is an optimal range for a power law. For example, at 2 M, the mean *a*-exponent for the 320-mer is 0.5. This could be passed off as just a fluctuation in the simulation results (around 0.4), but the general trend in Table 4 seems to be that the exponent has a minimum between 0.01 and 0.1 M. Note that there is no point in continuing with the Flory analysis to obtain ΔpK as was done in the salt-free case.[11] This would only lead to the nonphysical result $\Delta pK \propto 1/\alpha^{1/5}$.

Figure 12 describes the chain expansion upon an increase in pH for different amounts of added salt.

Table 3. R_{ee} Approximated as a Power Law: C_s-Exponents[a]

		α			
a/Å	*N*	0.25	0.50	0.75	1.0
3	80	−0.08	−0.10	−0.10	−0.10
	320	−0.20	−0.22	−0.23	−0.23
	1000	−0.25	−0.27	−0.27	−0.27
6	80	−0.10	−0.20	−0.15	−0.16
	320	−0.18	−0.22	−0.23	−0.24
	1000				
12	80	−0.09	−0.15	−0.14	−0.18
	320	−0.14	−0.19	−0.21	−0.22
	1000	−0.21	−0.24	−0.24	−0.26

[a] The value predicted by eq 21 is −0.2.

Table 4. R_{ee} Approximated as a Power Law: *a*-Exponents[a]

		α			
C_s/M	*N*	0.25	0.50	0.75	1.0
0.001	80	0.59	0.56	0.42	0.65
	320	0.38	0.38	0.27	0.46
	1000	0.24	0.22	0.10	0.25
0.010	80	0.52	0.43	0.43	0.45
	320	0.33	0.26	0.26	0.25
	1000	0.27	0.21	0.21	0.20
0.100	80	0.56	0.40	0.38	0.36
	320	0.41	0.32	0.32	0.30
	1000	0.37	0.31	0.22	0.29

[a] The value predicted by eq 21 is 0.4.

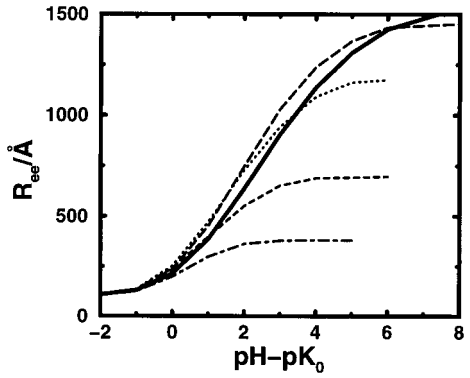

Figure 12. End-to-end separation as a function of pH − pK_0. The line types are as follows: long dashed line, 0.0001 M; dotted line, 0.001 M; short dashed line, 0.01 M; dot-dashed line, 0.1 M; and solid line, salt-free case. The bond length *a* is 6 Å, and the number of monomers *N* is 320.

Naively, one would always expect a contraction of the chain when salt is added to the system, due to the increased screening. One can note, however, that this is not always the case and that the addition of salt at constant pH may lead to an increased end-to-end separation. Similar behavior has been seen in other simulations.[2] Inclusion of attractive interactions will cause the transition between a random coil and extended rod seen in Figure 12 to appear over a more narrow pH interval, and it also seems to attenuate the anomalous salt effect on R_{ee}.

Experimentally, it has been observed that the helix content of poly-L-glutamic acid decreases when salt is added at constant pH (polyglutamic acid forms a helical conformation at low pH, when the polymer chain is neutralized).[33] We interpret this as a consequence of an increased ionization due to an increased screening upon the addition of salt. The global interactions are decreased and with them the electrostatic field at a titrating site, which can pick up more charge. This, on the other hand, leads to increased local interactions and

local expansions that can amount to a global expansion. The fact that it is observed in the simulations, Figure 12, tells us that the effect is originally of electrostatic origin, but it can, of course, be modulated by other interactions.

Conclusions

The present model, based on a uniform dielectric continuum approximation and with a screened Coulomb approximation for the electrostatic interactions, seems to capture some basic features of a titrating polyelectrolyte, even though it is too sensitive to the addition of salt in comparison to experiments. Within the Debye−Hückel approximation, a rigid rod can be successfully described with a mean field approximation, in which the charge is equally distributed as fractional charges on all the monomers, which shows that site−site correlations are of minor importance. An alternative approach, in which full charges are equally spaced, is less successful. Explicit treatment of nearest-neighbor correlations gives a small improvement at the expense of a greatly increased mathematical complexity.

The various rigid models that have been used over the years give little numerical differences within their range of validity, if the same value is used for all their length parameters. Since these parameters have different interpretations, the correspondence with physical reality becomes unclear. The rigid rod is strictly a one-parameter model, while the cylindrical surface, for example, can have two and even three parameters, which, of course, gives a certain fitting flexibility.

Compared to simulations of flexible chains, still within the Debye−Hückel approximation, the rigid models underestimate the absolute shift in the apparent dissociation constant, but they are able to describe its dependence on salt concentration and the bond length of the freely jointed chain. At large degrees of dissociation, they are also able to describe the slope of ΔpK *vs* α. For longer chains and moderate to high salt concentrations, ΔpK is independent of the number of monomers. Outside this range, an N-dependent form of the rigid rod can be used. At very low salt concentrations, however, other macroions and counterions start to contribute to the screening, and the screened Coulomb approximation becomes questionable.

Many variables enter in the comparisons with real systems, but some conclusions can still be reached. The simple model based on the Debye−Hückel approximation depends too strongly on the amount of salt. One probable reason is that the linear response, implied by the screened Coulomb potential, is not always valid. Some of the nonlinearity may be regained by solving the Poisson−Boltzmann equation. We managed to get good agreement by fitting the "linearized cylinder" to the data at low α and then solving the full Poisson−Boltzmann equation with the fitted parameters. On the other hand, the flexible model describes certain features of experimental curves, in particular the negative curvature at low degrees of ionization. We believe that, in this respect, the model is correct and gives some insight into the effects of flexibility. The use of hard spheres gives further clues to the effect of nonelectrostatic intramolecular interactions. We have also shown that a distance of closest approach, i.e., an excluded volume, with respect to the salt ions relieves some of the salt dependence and would improve the agreement of the flexible model with experiment. Attractive interactions would be necessary in order to model sharp structural transitions from helix to random coil or from a globular state to more extended conformations. Finally, we note that neither the Poisson−Boltzmann approximation nor the screened Coulomb potential accounts for ion−ion correlations. However, these are usually important only in the presence of multivalent counterions.

From a simple Flory argument, we managed to obtain a power law for the end-to-end separation that agrees remarkably well with simulations. We have also shown that the flexible model is able to produce the counterintuitive effect of an increased expansion on addition of salt which is observed experimentally.

Acknowledgment. Stimulating discussions with Carsten Peterson and Bo Söderberg are gratefully acknowledged. The codes for both the modified Bessel functions and the linear regression have been "borrowed" from *Numerical Recipes, The Art of Scientifics Computing*.[34] The Poisson−Boltzmann equation has been solved with a program written by Bengt Jönsson.

References and Notes

(1) Reed, C. E.; Reed, W. F. *J. Chem. Phys.* **1992**, *96*, 1609.
(2) Sassi, A. P.; Beltrán, S.; Hooper, H. H.; Blanch, H. W.; Prausnitz, J. M.; Siegel, R. A. *J. Chem. Phys.* **1992**, *97*, 8767.
(3) Chistos, G. A.; Carnie, S. L. *J. Chem. Phys.* **1989**, *91*, 439.
(4) Christos, G. A.; Carnie, S. L. *J. Chem. Phys.* **1990**, *92*, 7661.
(5) Hooper, H. H.; Blanch, H. W.; Prausnitz, J. M. *Macromolecules* **1990**, *23*, 4820.
(6) Hooper, H. H.; Beltran, S.; Sassi, A. P.; Blanch, H. W.; Prausnitz, J. M. *J. Chem. Phys.* **1990**, *93*, 2715.
(7) Christos, G. A.; Carnie, S. L.; Creamer, T. P. *Macromolecules* **1992**, *25*, 1121.
(8) Lal, M. *Mol. Phys.* **1969**, *17*, 57.
(9) Madras, N.; Sokal, A. D. *J. Stat. Phys.* **1988**, *50*, 109.
(10) Ullner, M.; Jönsson, B.; Widmark, P.-O. *J. Chem. Phys.* **1994**, *100*, 3365.
(11) Ullner, M.; Jönsson, B.; Söderberg, B.; Peterson, C. *J. Chem. Phys.* **1996**, *104*, 3048.
(12) Manning, G. S. *J. Phys. Chem.* **1981**, *85*, 870.
(13) Cleland, R. L.; Wang, J. L.; Detweiler, D. M. *Macromolecules* **1984**, *17*, 634.
(14) Hill, T. L. *Arch. Biochem. Biophys.* **1955**, *57*, 229.
(15) Nagasawa, M.; Holtzer, A. *J. Am. Chem. Soc.* **1964**, *86*, 531.
(16) Cleland, R. L.; Wang, J. L.; Detweiler, D. M. *Macromolecules* **1982**, *15*, 386.
(17) Manning, G. S. *J. Chem. Phys.* **1969**, *51*, 924.
(18) Manning, G. S.; Holtzer, A. *J. Phys. Chem.* **1973**, *77*, 2206.
(19) Manning, G. S. *Acc. Chem. Res.* **1979**, *12*, 443.
(20) Kawaguchi, Y.; Nagasawa, M. *J. Phys. Chem.* **1969**, *73*, 4382.
(21) Mandel, M. *Eur. Polym. J.* **1970**, *6*, 807.
(22) Olander, D. S.; Holtzer, A. *J. Am. Chem. Soc.* **1968**, *90*, 4549.
(23) Muroga, Y.; Suzuki, K.; Kawaguchi, Y.; Nagasawa, M. *Biopolymers* **1972**, *11*, 137.
(24) Kotin, L.; Nagasawa, M. *J. Chem. Phys.* **1962**, *36*, 873.
(25) Ullner, M.; Woodward, C. E.; Jönsson, B. *J. Chem. Phys.* **1996**, *105*, 2056.
(26) Metropolis, N. A.; Rosenbluth, A. W.; Rosenbluth, M. N.; Teller, A.; Teller, E. *J. Chem. Phys.* **1953**, *21*, 1087.
(27) Marcus, R. A. *J. Phys. Chem.* **1954**, *58*, 621.
(28) Harris, F. E.; Rice, S. A. *J. Phys. Chem.* **1954**, *58*, 733.
(29) Nagasawa, M.; Murase, T.; Kondo, K. *J. Phys. Chem.* **1965**, *69*, 4005.
(30) Bret, M. L.; Zimm, B. H. *Biopolymers* **1984**, *23*, 287.
(31) de Gennes, P. G. *Scaling Concepts in Polymer Physics*; Cornell University Press: Ithaca, NY, 1979.
(32) de Gennes, P. G.; Pincus, P.; Velasco, R. M.; Brochard, F. *J. Phys.* **1976**, *37*, 1461.
(33) Nilsson, S.; Zhang, W. *Macromolecules* **1990**, *23*, 5234.
(34) Press, W. P.; Flannery, B. P.; Teukolsky, S. A.; Vettering, W. T. *Numerical Recipes, The Art of Scientific Computing*; Cambridge University Press: Cambridge, UK, 1986.

MA960309W